文章编号：0258-7025(2009)12-3179-13

Direct Manufacturing of Net-Shape Functional Components by Laser Consolidation Process

(Invited Paper)

Lijue Xue

(*Industrial Materials Institute, National Research Council of Canada*
800 *Collip Circle, London, Ontario, N6G 4X8, Canada*)

Corresponding author: lijue.xue@nrc-cnrc.gc.ca

Received October 13, 2009

Abstract Laser consolidation (LC) is a novel computer-aided manufacturing process developed by the Industrial Materials Institute of National Research Council of Canada (NRC-IMI). This rapid manufacturing process produces net-shape functional metallic parts layer-by-layer directly from a computer aided design (CAD) model by using a laser beam to melt the injected powder and re-solidifying it on the substrate or previous layer. As an alternative to the conventional machining process, this novel manufacturing process builds net-shape functional parts or features on an existing part by adding instead of removing material. In this review paper, LC of CPM-9V tool steel, Ni-based IN-625 and IN-718 superalloys, and Ti-6Al-4V alloy will be discussed. The microstructures and functional properties of these laser consolidated materials will be examined along with several potential industrial applications.

Key words laser direct manufacturing; laser consolidation; net-shape; rapid manufacturing; green manufacturing

CLCN: TN249;TG146.4 **Document Code**: A **doi**: 10.3788/CJL20093612.3179

1 Introduction

Laser cladding based free-form fabrication is an emerging computer-aided manufacturing technology that uses a laser beam to melt injected powder (or wire) to form a solid, functional component layer by layer. This one-step computer-aided manufacturing process does not require any mould or die, and therefore provides the flexibility to quickly change the design of the components. As a result, the lead-time to produce functional parts could be reduced significantly. As opposed to the conventional machining process, this new technology builds complete parts or features on an existing component by adding rather than removing material. The parts built by the laser deposition process are metallurgically sound and free of porosity or cracks. The research works have been reported by various institutions using laser cladding based free-form fabrication technology on various alloys and steels[1~4]. Although the technology has a great potential for many industrial applications, concerns about the surface finish and dimensional accuracy have been raised.

The Industrial Materials Institute of National Research Council of Canada (NRC-IMI) has been developing laser consolidation (LC) process that takes the laser cladding based free-form fabrication technology to a new level enabling production of net-shape functional components, and such components are difficult or even impossible to produce using conventional manufacturing technologies[5]. The research works have been published on LC of various industrial materials (such as Ni-alloys, Co-alloys, Ti-alloys, Al-alloys, stainless steels, and tool steels)[5~10] and its potential for various industrial applications[11~15]. In this review paper, LC process is introduced, the microstructures and functional properties of several laser-consolidated materials are described, several case studies are presented, and the potential applications of the process for manufacturing net-shape functional components are discussed.

2 Experimental Details

LC process requires a substrate (new base or on existing component) onto which a part is built (Fig. 1). A focused laser beam is irradiated on the substrate to create a molten pool, while metallic powder through a nozzle is injected simultaneously into the pool. A numerically controlled (NC) motion system (3 to 5 axes) is used to control the relative movement between the laser beam and the substrate. The laser beam and the powder feed nozzle

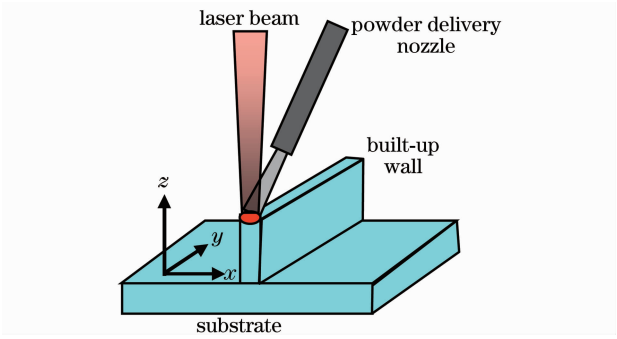

Fig. 1 Illustration of laser consolidation process

are moved following a computer aided design (CAD) model through a pre-designed laser path, creating a bead of molten material on the substrate, which solidifies rapidly to form the first layer. The second layer is deposited on the top of the first layer. By repeating this process, a solid thin walled structure is built. When the laser path is designed properly to guide the laser beam movement, a complex shaped part can be built directly from a CAD model without any mould or die.

LC process presented in this paper was conducted using a proprietary LC system developed by NRC - IMI. A 500-W or 1-kW LASAG Nd∶YAG laser coupled to a fiber-optic processing head was used for the experiments. The laser was operated in a pulse mode with the average powers ranging from 20 to 300 W. A Sultz-Metco 9MP powder feeder was used to simultaneously deliver metallic powder into the melt pool through a nozzle with the powder feed rates ranging from 1 to 30 g/min. A 4- or 5-axis NC motion system was used for LC process, while processing was conducted in a glove box, in which the oxygen content was maintained below 50 ppm during the process.

Chemical compositions of the four alloy powders investigated in this paper, Ni-base IN-625 and IN-718 alloys, Ti-base Ti-6Al-4V alloy, and CPM-9V tool steel, are listed in Table 1. Annealed A36 mild steel plates (0.29% C, 1.0% Mn, 0.2% Cu, and Fe) with a thickness of 12.7 mm were used as the base material for LC of IN-625, IN-718, and CPM-9V materials, while wrought Ti-6Al-4V alloy substrate was used for LC of Ti-6Al-4V alloy. The substrate plates were machined and ground to a consistent surface finish for the laser consolidation of different alloy powders.

Table 1 Chemical compositions of alloy powders (mass fraction, %)

Alloy	C	Ni	Ti	Fe	Al	Cr	Mo	Ta + Nb	V	Mg	Si
IN-625	0.03	Bal.	–	–	–	22.0	9.0	3.7	–	–	–
IN-718	0.05	Bal.	–	17.0	–	19.0	3.0	5.0	–	–	–
Ti-6Al-4V	0.07	0.02	Bal.	–	6.18	0.02	–	–	3.94	–	–
CPM-9V	1.8	–	–	Bal.	–	5.35	1.24	–	9.26	0.5	0.91

The microstructures of the LC samples were examined using an Olympus optical microscope as well as a Hitachi S-3500 scanning electron microscope (SEM). A Philips X'Pert X-ray diffraction (XRD) system was used to identify the phases of the LC materials. A 100 kN Instron mechanical testing system was used to evaluate the tensile properties and fatigue lives of the LC samples, while the sliding wear resistance of LC CPM-9V was evaluated using a Falex pin-on-disk tester against a 6.35-mm (1/4″) diameter WC ball (HRa 92). Wear testing was conducted under a normal load of 500 g with a linear speed of 0.28 m/s running for a total sliding distance of 8000 m. The microhardness of clad materials was measured using a Buehler Micromet II microhardness tester.

3 Microstructures and Properties of Several LC Materials

3.1 LC CPM-9V Tool Steel

CPM-9V is a vanadium-carbide enhanced tool steel developed by Crucible Research for powder metallurgy applications. As compared to conventional tool steels, CPM-9V exhibits the excellent wear resistance[16]. CPM-9V is suitable for use in tooling which encounters severe wear, such as forming rolls, rolling mill rolls, header tooling, extrusion tooling, punches, dies, shear blades, etc.

With the optimized processing parameters, the LC CPM-9V material is fully dense, free of cracks and porosity[11]. LC CPM-9V has a very fine microstructure, which is very hard to identify under optical microscope. A high resolution SEM photo (Fig. 2(a)) shows that the as-consolidated CPM-9V has two-phase microstructure: a light, very fine and snowflake-like phase precipitated on the dark matrix. The thickness of the light snowflake-like phase is only about 100 nm (Fig. 2(b)). EDS analysis indicates that the light phase contains higher percentage of vanadium (about 12% ~ 14%) and

chromium (about 6% ~ 6.6%) as compared to the dark matrix (about 9% V and 5.7% Cr). The XRD analysis further reveals that the light phase is $(V, Cr)_8C_7$ type carbides, while the dark one is α phase.

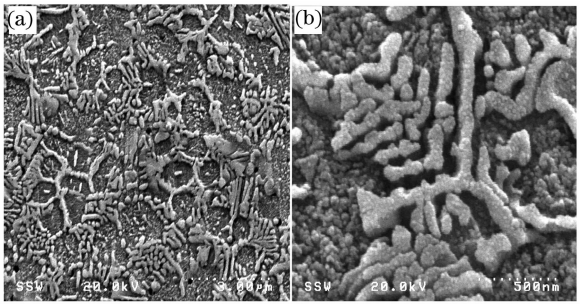

Fig. 2　SEM microstructure of LC CPM-9V
(a) 6500×; (b) 40000×

The LC CPM-9V material shows the very good tensile properties (Table 2). Along the vertical (build-up) direction, the as-consolidated CPM-9V has average yield strength ($\sigma_{0.2}$) of 821 MPa and tensile strength (σ_{UTS}) of 1315 MPa. The elastic modulus (E) of the consolidated CPM-9V is about 234 GPa. Unfortunately, all specimens failed outside of the gauge length, and therefore the accurate elongation data are not available. But based on the measured data within the gauge length, the average elongation (δ) of the as-consolidated CPM-9V is above 2.6%. It should be noted that all the tensile test data are very consistent and the scattered ranges are small, which indicates that LC process has the good reproducibility.

Table 2　Tensile properties of LC CPM-9V tool steel

Sample No.	σ_{UTS} /MPa	$\sigma_{0.2}$ /MPa	δ /%	E /GPa
#1	1358.9	883.8	2.3*	229.6
#2	1295.0	787.0	2.8*	230.6
#3	1303.8	835.9	2.2*	244.5
#4	1303.8	778.1	3.1*	232.7
Average	1315 ± 29	821 ± 49	2.6*	234 ± 7

LC CPM-9V also shows the excellent sliding wear resistance (Fig. 3). Pin-on-disk testing reveals that, under the given test conditions (tested against 6.35-mm diameter WC ball under 500-g load at a linear speed of 0.28 m/s for a total distance of 8000 m), the LC CPM-9V specimens (Rc. 50-55) shows the significantly better wear resistance as compared to hardened D2 steel (Rc. 64-65) and normalized 4340 steel (Rc. 35-36). The average volume loss of the LC CPM-9V specimens was about 0.0211 mm^3, which was only about 1/3 of the volume loss of the D2 specimens (0.0595 mm^3) and about one order of magnitude lower as compared to

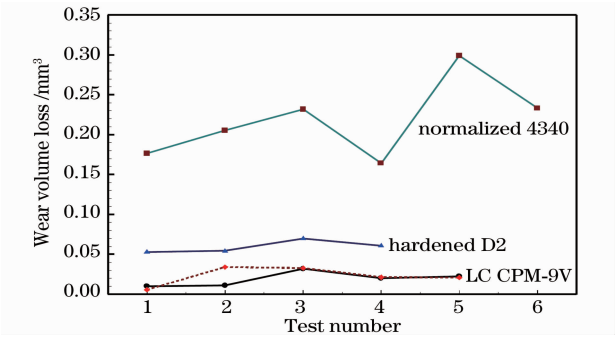

Fig. 3　Pin-on-disk wear testing results
(disk volume loss)

the 4340 specimens (0.2185 mm^3).

In addition, the wear loss of the WC balls tested against the LC CPM-9V material was also significantly lower than that of the same balls against the D2 and 4340 steels. The average wear volume loss of the WC balls against the LC CPM-9V was only about 0.01855 mm^3, while the ball volume loss against the D2 and 4340 steels was increased double and triple (0.0417 and 0.0538 mm^3), respectively.

It is interesting to note that although the hardness of the as-consolidated CPM-9V material is only around Rc. 50-55, its wear resistance is clearly superior to the hardened D2 steel with a hardness of around Rc. 64-65, which is consistent with the observation on powder metallurgy (P/M) CPM-9V material[16]. The excellent wear resistance of LC CPM-9V may be attributed to the precipitation of $(V, Cr)_8C_7$ carbides due to the high vanadium contents in the alloy.

3.2　LC IN-625 Alloy

IN-625 is a solution-hardenable nickel-chromium superalloy containing molybdenum, tantalum, and niobium alloying elements. It has the excellent corrosion and oxidation resistance, outstanding strength and toughness in the temperature range up to 1093 ℃ (2000 ℃). The alloy has the excellent fatigue strength and stress-corrosion cracking resistance to chloride ions. IN-625 alloy has been used to manufacture components for gas turbine engine ducting, combustion liners and spray bars, heat shields, furnace hardware, chemical plant hardware, special seawater applications, etc[17].

LC of IN-625 powder produces metallurgically sound components, free of cracks or porosity. Figure 4 shows three LC IN-625 samples: a hollow square, a hollow cylinder, and a hollow cone. These samples were prepared for measurement of the surface roughness as well as the dimensional ac-

curacy. It is evident that LC IN-625 samples show the very good surface finish. Surface roughness measurement reveals that the average roughness (R_a) of the as-consolidated IN-625 samples is about 1.5～1.8 μm[5].

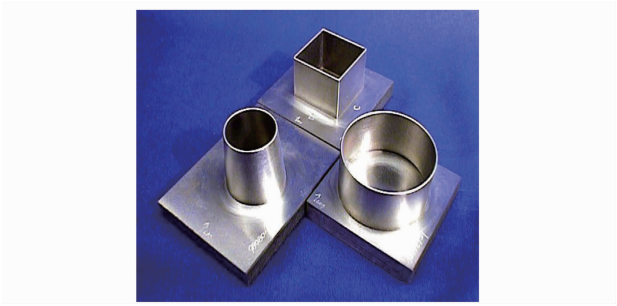

Fig. 4 Three as-consilidated LC IN-625 samples

The LC samples have the very good dimensional accuracy. For the hollow square (25 mm × 25 mm), the standard deviations in the wall thickness and height are only about 0.025 and 0.038 mm, respectively, while the wall parallelism is within the range of 0.050 mm. The average squareness between walls is 90.00° with a deviation of 0.02°, while the average perpendicularity of the square walls against the base plate is 89.92°. For the cylinder, the standard deviations in the inner and outer diameters are within 0.050 mm. For both the thin-wall cylinder and the cone, the deviations in circularity are less than 0.050 mm, while the deviations in cylindricity and conicity are 0.086 and 0.069 mm, respectively. It is notable that the measurement of the inclined angle for the built cone is 9.93° compared to the required 10°. These errors could be attributed to the repeatability errors in the motion system as well as the errors caused by LC itself.

The LC IN-625 material shows the unique directionally solidified microstructure due to the rapid solidification inherent to the process (Fig. 5). The cross-sectional view along the vertical direction shows that LC IN-625 has columnar grains growing almost parallel to the build-up direction (Fig. 5 (a)), while the horizontal (perpendicular to the build-up) cross section shows that the LC IN-625 consists of fine cells of around 2～3 μm in diameter (Fig. 5(b)). The XRD reveals that the LC IN-625 has the same γ phase as the IN-625 powder: a face-centered cubic structure with a lattice parameter of 0.359 nm. The directional solidification of the LC IN-625 material is along the (100) crystallographic plane, which is the typical dendritic growth direction of the face-centered cubic structure materials[18].

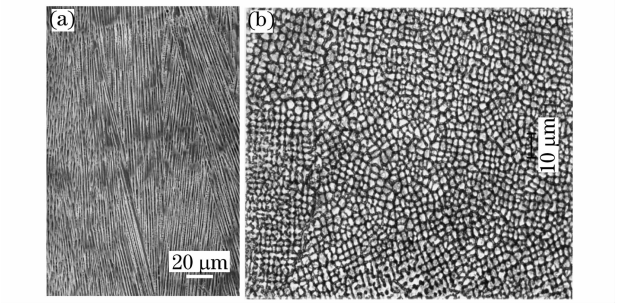

Fig. 5 Microstructure of LC IN-625 alloy. (a) vertical cross-sectional view; (b) horizontal cross-sectional view

The LC IN-625 material exhibits the good mechanical properties (Table 3). Along the horizontal direction, the yield and tensile strengths of the LC IN-625 material are 518 and 797 MPa, respectively, while the elongation is about 31%. When testing along the vertical direction, both the yield and the tensile strengths are slightly reduce to 477 and 744 MPa, respectively, while the percentage elongation increases significantly to 48%. The anisotropic behaviour of the tensile properties of LC IN-625 alloy may be attributed to its directionally solidified microstructure. The yield and the tensile strengths of LC IN-625 along both directions are significantly higher than the cast IN-625 and comparable to the wrought material, although the elongation along the horizontal direction is slightly lower.

Table 3 Tensile properties of LC IN-625 alloy

Conditions		$\sigma_{0.2}$ /MPa	σ_{UTS} /MPa	δ /%
LC IN-625	Horizontal	518 ± 9	797 ± 8	31 ± 2
(as-consolidated)	Vertical	477 ± 10	744 ± 20	48 ± 1
As-cast IN-625[19]		350	710	48
Annealed wrought IN-625[20]		490	855	50

The results of the fatigue tests at room temperature are displayed in Fig. 6[21]. The LC IN-625 material tested in the vertical direction had a fatigue resistance significantly higher than the investment cast but lower than the wrought material. The endurance limit of the LC material was just under 450 MPa, which is about 200 MPa higher than the investment cast material and about 100 MPa lower than the wrought material. There was essentially no difference in the fatigue resistance between the two orthogonal directions (A and B) on wrought IN-625 sheet. In addition, the stress relieving (SR)

treatment did not affect the fatigue resistance of the wrought material.

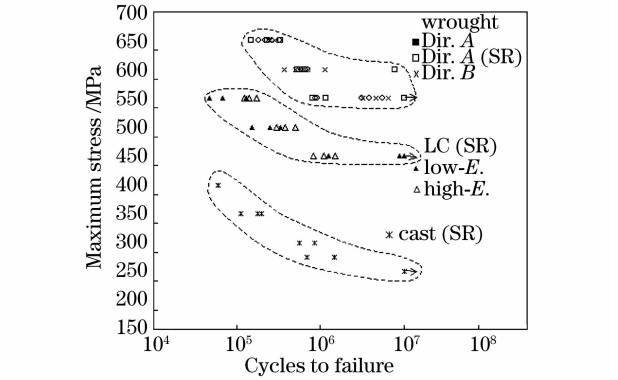

Fig. 6　Fatigue testing results of IN-625 under a stress-controlled sinusoidal waveform ($R = 0.1$, $f = 60$ Hz)

In principle, LC process is a form of casting process where the material is melted and re-solidified in order to form a desired shape. The LC IN-625 material has essentially a cast microstructure. However, due to the rapid solidification inherent to the process, LC microstructure is much more refined and uniform than the investment cast material. Furthermore, the LC material is free of cracks and porosity. This proved to be beneficial for the room temperature fatigue properties.

3.3　LC IN-718 Alloy

IN-718 is a precipitation-hardenable nickel-chromium superalloy containing significant amounts of iron, niobium, and molybdenum, along with lesser amount of aluminum and titanium. It combines the good corrosion resistance and the high strength with outstanding weldability, including the resistance to post-weld cracking. The alloy has the excellent creep-rupture strength at temperature up to 700 ℃ (1300 ℃). IN-718 has been widely used as a structural material for a variety of components in gas turbines, rocket motors, spacecraft, nuclear reactors, pumps, and tooling[22].

LC processing parameters were successfully developed to build IN-718 samples with the good repeatability and high integrity[10]. Similar to LC IN-625, the as-consolidated IN-718 also shows directionally solidified microstructure due to the rapid solidification inherent to LC process (Fig. 7). The cross-sectional view shows that the as-consolidated IN-718 has columnar dendritic grains growing almost parallel to the vertical direction (Fig. 7(a)), while the horizontal cross section shows fine cell structure (Fig. 7(b)).

The standard heat treatment procedure used

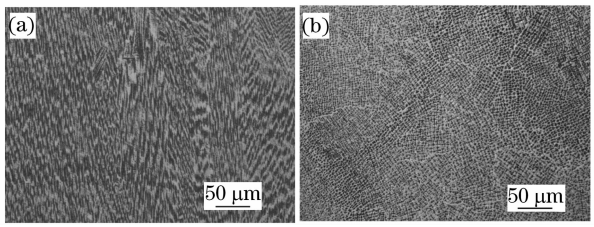

Fig. 7　Optical microstructure of the as-consolidated IN-718 (a) vertical direction; (b) transverse direction, 100×

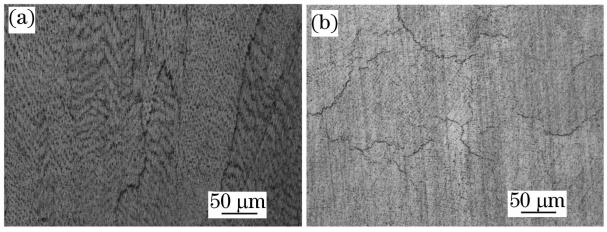

Fig. 8　Microstructure of HT LC IN-718 (a) vertical direction; (b) transverse direction, 200×

for wrought IN-718 was also applied for LC IN-718 specimens: 1) solution treatment at 980 ℃ for 1 h followed by air cooling; 2) aging at 720 ℃ for 8 h followed by air cooling, and 3) aging at 620 ℃ for 8 h followed by air cooling. Figures 8(a) and (b) show optical microscopic photos of the heat-treated (HT) LC IN-718 along the vertical and horizontal directions, respectively. After the heat treatment, the original columnar dendrites in LC IN-718 disappeared.

However, it is interesting to note that some kinds of dendritic features can still be observed under optical microscope in HT LC IN-718 (Fig. 8 (a)). High resolution SEM observation reveals that those features can be attributed to carbide particles existing in the prior inter-dendritic regions and no dendritic structures remained after the heat treatment. For the as-consolidated IN-718, no γ' particles can be observed. After the standard heat treatment, γ' particles precipitated in the LC IN-718 matrix, as indicated by the significant increase in its hardness (from HV 257 increased to HV 445). However, we did not observe γ' particles under SEM with the current reagent. The work is still in progress and the results will be published later.

The XRD (Fig. 9) reveals that the as-consolidated IN-718 has the same γ phase as the IN-718 powder: a face-centered cubic structure. However, the as-consolidated IN-718 material shows a preferred orientation along the (100) crystallographic plane (the typical dendritic growth direction of face-centered cubic structure materials). It is in-

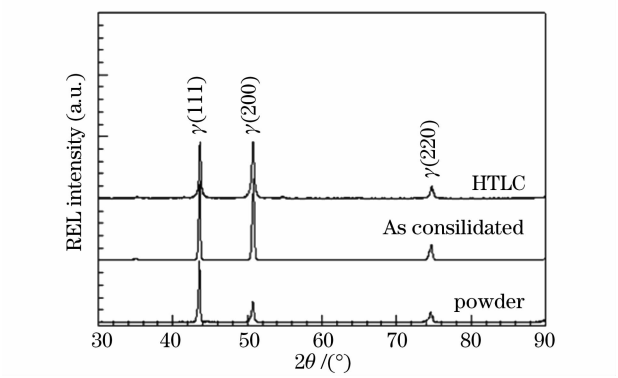

Fig. 9 XRD patterns of powder, as-consolidated and HT LC IN-718

teresting to note that, after heat treatment, the preferred orientation along (100) still remained, although its original dendrites disappeared.

LC successfully produced metallurgically sound IN-718 samples, free of cracks or porosity. Due to the time limitation, we only investigated the mechanical properties of LC IN-718 alloy along the vertical direction. Table 4 compares the tensile properties of LC IN-718 with various wrought IN-718 materials. The as-consolidated IN-718 alloy shows the reasonably good tensile properties. The average yield and ultimate tensile strengths of the as-consolidated IN-718 are about 432 and 802 MPa, respectively, while the elongation is about 39%. It should be noted that the tensile properties of the LC IN-718 material have relatively small scatter. The standard deviations of yield and ultimate tensile strengths are only 5 and 21 MPa, respectively, while the standard deviation of the elongation is about 5%, which indicates that LC IN-718 material has the good consistency.

Table 4 Tensile properties of LC IN-718 alloy

Material	$\sigma_{0.2}$ / MPa	σ_{UTS} / MPa	δ / %
LC IN-718 (as-consolidated)	432 ± 5	802 ± 21	39 ± 5
LC IN-718 (HT)	1085 ± 19	1238 ± 12	21 ± 2
Wrought IN-718 (HT)[22]	1036	1240	12
IN-718 Sheet (HT)[23]	1050	1280	22
IN-718 Bar (HT)[23]	1190	1430	21

After the heat treatment, the yield and tensile strengths of the LC IN-718 was increased to about 1085 and 1238 MPa, respectively, while the elongation was reduced to about 21% (Table 4). The HT LC IN-718 alloy demonstrates that its yield and tensile strengths, and elongation are comparable to the various types of HT wrought IN-718 material. The microhardness of LC IN-718 is about HV 257 and HV 445 for as-consolidated and HT conditions, respectively, while the hardness of HT wrought IN-718 is about HV 420[24].

The state of residual stresses in the LC IN-718 material was measured using conventional XRD method. It reveals that the surface residual stress along the horizontal direction of the as-consolidated IN-718 is in compression (about -297 ± 15 MPa), while it is in tension along the vertical direction (about $+121 \pm 12$ MPa). After heat treatment, the residual stresses along the horizontal direction remains in compression (-245 ± 25 MPa), while the residual stresses along the vertical direction is completely eliminated (about -3 ± 66 MPa). It should be noted that the existence of compressive residual stress in the HT LC IN-718 will be beneficial to its potential application for making gas turbine engine components.

3.4 LC Ti-6Al-4V Alloy

Ti-6Al-4V is known as the "workhorse" of titanium industry, accounting for more than 50% of total titanium usage. It is an $(\alpha+\beta)$ alloy that offers a good combination of high strength, light weight, formability and corrosion resistance. Ti-6Al-4V is recommended for use at service temperature up to 350 ℃. It has been used for making aircraft turbine engine components, aircraft structural components, high-performance automotive parts, marine applications, medical devices, sports equipment, etc[25].

The LC Ti-6Al-4V material is metallurgically sound. Figure 10 reveals the microstructure of the LC Ti-6Al-4V along the vertical cross-section[8]. The LC Ti-6Al-4V shows somewhat equiaxed grains (Fig. 10(a)) with acicular phase inside (Fig. 10(b)). A high-resolution SEM photo reveals that grain boundary is hard to distinguish and no secondary phase can be observed along it (Fig. 10(c)).

Ti-6Al-4V is an $(\alpha+\beta)$ alloy and its typical as-cast microstructure consists of transformed β containing acicular α as well as α at prior-β grain boundaries, while the annealed wrought Ti-6Al-4V bar typically consists of equiaxed α grain plus intergranular β[26]. XRD technique was used to identify the phases in the wrought, powder, and LC Ti-6Al-4V. It can be seen from Fig. 11 that wrought Ti-6Al-4V has majority of α phase plus small amount of β phase evidenced by the existence of $\beta(200)$ peak as well as shape changes of $\alpha(101)$ and $\alpha(103)$ peaks caused by $\beta(110)$ and $\beta(211)$ peaks, respectively. It is inter-

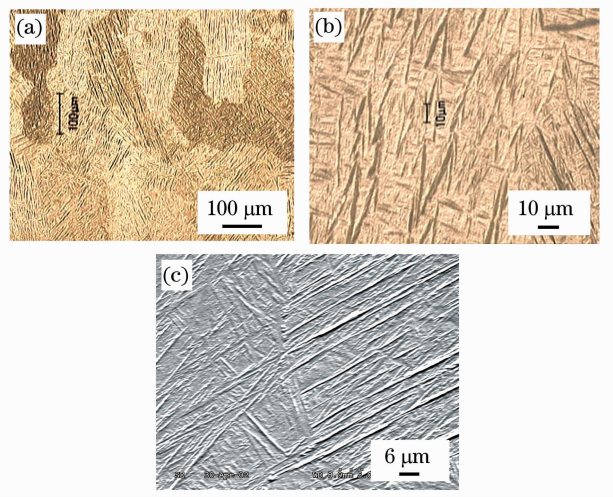

Fig. 10　Microstructure of LC Ti-6Al-4V. (a) optical micrograph, 100 ×; (b) optical micrograph, 1000 ×; (c) SEM micrograph, 1500 ×

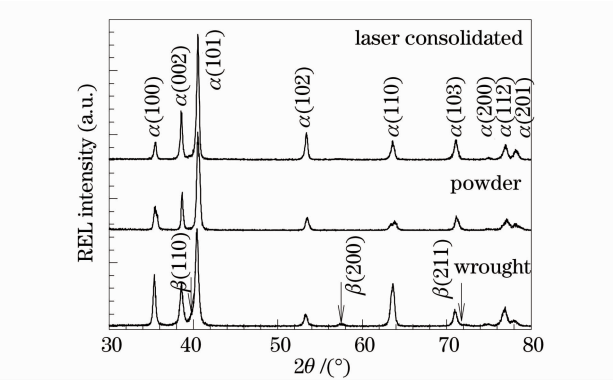

Fig. 11　XRD patterns of wrought, powder and LC Ti-6Al-4V

esting to note that the powder Ti-6Al-4V material shows only α phase, presumably due to the rapid solidification inherent to the gas atomization process used for producing the powder.

LC Ti-6Al-4V has the same phase structure as the powder used: single α-phase microstructure with $\alpha(101)$ as the strongest diffraction peak without any β peaks, which is consistent to the optical microscope and SEM observations. Similar to the powder Ti-6Al-4V, the lack of β phase in LC Ti-6Al-4V may also be attributed to the high cooling rate inherent to the process. Based on the optical microscope, SEM, and XRD results, LC Ti-6Al-4V microstructure consists of somewhat equiaxed α grains (transformed from β) with acicular features inside.

The LC Ti-6Al-4V material exhibits the very good mechanical properties. The tensile properties of the as-consolidated Ti-6Al-4V materials tested at room temperature are listed in Table 5[30]. The yield and tensile strengths of the thin-wall (0.8-mm thick) LC Ti-6Al-4V material are 1062 and 1157 MPa, respectively, while its elongation in 25-mm gauge length is 6.2%. Both tensile and yield strengths of the thin-wall LC Ti-6Al-4V are substantially higher than the as-cast/annealed cast Ti-6Al-4V and annealed wrought Ti-6Al-4V, and comparable to the HT wrought Ti-6Al-4V (in solution treated plus aged condition). The elastic modulus of the thin-wall LC Ti-6Al-4V (116 GPa) is comparable to the wrought material (110 GPa). However, the elongation of the LC material (6.2%) is lower than the cast or wrought Ti-6Al-4V (8% ~ 10%).

Table 5　Tensile properties of LC Ti-6Al-4V alloy

Materials	$\sigma_{0.2}$ /MPa	σ_{UTS} /MPa	E /GPa	δ /%
As-consolidated Ti-6Al-4V (thick-wall)	899	979	121	11.4
As-consolidated Ti-6Al-4V (thin-wall)	1062	1157	116	6.2
As-cast Ti-6Al-4V[27]	890	1035	–	10
Wrought Ti-6Al-4V (annealed)[28]	825	895	110	10
Wrought Ti-6Al-4V (solution treated and aged bar)[28]	965	1035	110	8
Wrought Ti-6Al-4V (solution HT and aged)[29]	1103	1172	–	10

The thick-wall (1.5-mm thick) LC Ti-6Al-4V material was found to have the slightly lower tensile and yield strengths but a higher ductility than the thin-wall LC material. The average yield and tensile strengths of this material in the as-consolidated condition are 899 and 979 MPa, respectively. The average elongation is around 11.4% and the elastic modulus is slightly higher at around 121 GPa. The tensile properties of the thick-wall LC Ti-6Al-4V are comparable to the as-cast (or annealed) cast Ti-6Al-4V material and better than the annealed wrought Ti-6Al-4V material.

The results of high-cycle fatigue testing are displayed in Fig. 12. Both the thin-wall and thick-wall LC Ti-6Al-4V specimens were tested in as-consolidated condition at room temperature. As a preliminary study, only five thick-wall LC Ti-6Al-4V specimens were tested to determine how the fatigue

properties of LC Ti-6Al-4V are affected by the LC process parameters. The plot also shows the reference data for cast, cast plus HIP and annealed wrought Ti-6Al-4V[31] for comparison purposes. The endurance limit shown by the thin-wall LC Ti-6Al-4V specimens is around 400 MPa, which is at the high end of the cast material scatter band. The preliminary tests conducted on the thick-wall LC Ti-6Al-4V specimens have demonstrated a significant improvement in fatigue resistance over the thin-wall specimens. The results show that the endurance limit of the thick-wall LC Ti-6Al-4V material is in excess of 500 MPa, which is well within the scatter band of annealed wrought material. These preliminary results are very promising and demonstrate that the adjustment of LC processing parameters can significantly improve the fatigue properties of LC Ti-6Al-4V.

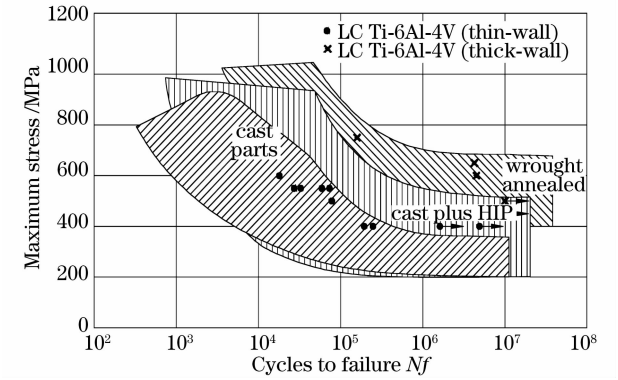

Fig. 12 Fatigue data of LC Ti-6Al-4V as compared with cast and wrought/anneal Ti-6Al-4V ($R = +0.1$)[30]

4 Some Case Studies for Industrial Applications

4.1 Rotary Cutting Dies

For many applications, rotary cutting dies are very efficient and commonly used by the industry. These high-volume, high-speed cutting dies are used for cutting a wide range of materials, such as labels, sand paper, carpet and fabric, from roll stocks, or directly in-line with printing and processing equipment, resulting in a dramatic increase in the productivity and cost savings. The manufacturing of these rotary cutting dies, however, is costly and time-consuming. Depending on the complexity of the cutting pattern and the height of the cutting blades, entire manufacturing process may take several days or even weeks to complete. The LC process provides an exceptional capability to manufacture the rotary dies by building up cutting blades instead of machining them out from the expensive tool steel stock. With this process, wear resistant materials can be used to build up the cutting blades on a low cost steel blank without the need of heat treatment. Thus, the consolidation process could significantly reduce the lead-time in the manufacturing of cutting die along with an improvement in its life. LC of CPM-9V was investigated in collaboration with Rotoflex International for manufacturing cutting blades on low-cost steel substrate[11].

LC process was developed to build CPM-9V cutting blades on the low alloy steel base for rotary cutting die application. With the optimized processing parameters, LC CPM-9V blades are fully dense, free of cracks and porosity. A rectangular cutting pattern (Fig. 13) was manufactured by LC of CPM-9V material on a flat base for the dimensional accuracy measurements. The measurements were performed by using a Mitutoyo microscope equipped with an x-y stage. Three points on each wall were selected to measure the wall thickness as well as the distance between the walls.

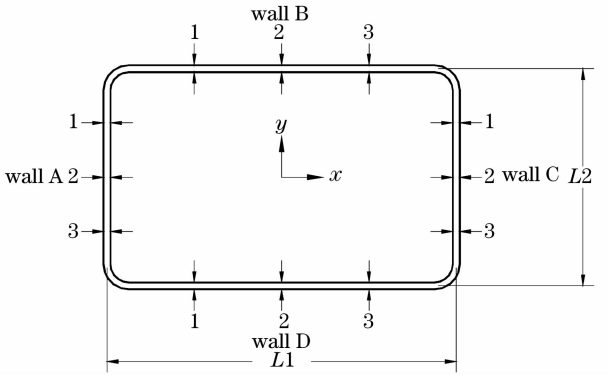

Fig. 13 Details of dimensions taken for measurement on a laser consolidated rectangular cutting pattern

The measurement results (Table 6) show that the distance between walls is very uniform. The standard deviations of the three measurements for distance $L1$ and $L2$ is only about 0.028 and 0.005 mm, respectively, and the difference between the laser consolidated wall and the CAD design is only about 0.030 mm for both cases. The wall thickness is very uniform with the standard deviations only from 0 to 0.046 mm. However, there are some slightly thickness differences between walls. The thickness of thickest wall D is about 1.153 mm, while the thinnest wall C is only about 0.927 mm, leaving the maximum thickness differ-

ence between walls of about 0.226 mm. Because all laser-consolidated walls will be finish machined, the thickness difference will not affect the sharpening of the cutting blades as long as the distance between walls, and the wall thickness are within the acceptable range.

Table 6 Dimensional measurement results (unit: mm)

Dimension	Measurements			Average	Std. Deviation	Nominal	Difference
	Position 1	Position 2	Position 3				
Wall thickness measurement							
Wall A	0.996	1.034	1.036	1.021	0.023	-	-
Wall B	1.143	1.143	1.143	1.143	0.000	-	-
Wall C	1.001	1.008	0.927	0.978	0.046	-	-
Wall D	1.153	1.146	1.153	1.151	0.005	-	-
Wall distance measurement							
$L1$	50.744	50.764	50.800	50.770	0.028	50.800	-0.030
$L2$	31.463	31.463	31.471	31.466	0.005	31.496	-0.030

Various types of rotary cutting dies have been successfully made by using LC process to build CPM-9V cutting blades on low cost blanks. Figure 14 shows a laser-consolidated rotary cutting die after the final sharpening. Field production testing shows that the LC CPM-9V rotary cutting dies have successfully cut more than 180000 m of labels without re-sharpening, while the dies made by D2 tool steel usually need re-sharpening after running the same period.

Fig. 14 LC CPM-9V rotary cutting die after final sharpening

Based on our industrial partner's estimation, LC process has the potential to manufacture rotary cutting dies with reducing the manufacturing time by 1/3 (for dies larger than 127 mm in diameter), reducing the material cost by approximately 50%, and increasing the cutting die life by approximately 100%. In addition, with this process, worn-out cutting blades could be repaired or the same blank could be reused for building a new cutting pattern after machining out the old pattern. Die blanks can be recycled to reduce environmental impaction.

4.2 Structural Components for ARMS

Advanced robotic mechatronics system (ARMS) project was initiated by MD Robotics and supported by the Canadian Space Agency (CSA). The main objective of this project was to investigate the use of enabling and emerging technologies for the design and manufacture of the next generation space robotic arms. In collaboration with MD Robotics and CSA, NRC-IMI utilized LC as a rapid manufacturing technology to make functional prototypes of structural components for ARMS[12].

One goal of ARMS project was to develop a multifunctional boom structure capable of providing high structural stiffness, with dedicated features to support electronic driver/control cards and the data/power bus while allowing the dissipation of the heat generated by the electronic drivers.

Three boom shapes were initially designed: boom design #1 has an inside slot to hold an electronic board plus four external slots to hold wires. Boom design #2 has a slot to hold an electronic board plus an enclosed tube to hold wires inside the boom, while boom design #3 has a slot to hold an electronic board (Fig. 15). All three designs provide the support for the electronic board as well as the heat dissipation. However, these multi-function, thin-walled structural components are difficult to manufacture using conventional technologies.

LC process provides an unique rapid manufacturing capability to make net-shape functional prototypes to materialize these innovative designs. Figure 16(a) shows the boom design #1 built by using LC of IN-625 alloy. Figures 16(b) and (c) show the laser consolidated IN-625 boom design #2 with slots formed by ribs and rectangular tubes, respectively. It is obvious that LC process generates high-quality functional prototypes for multi-functional boom structures that are difficult to make by using conventional manufacturing technology. This

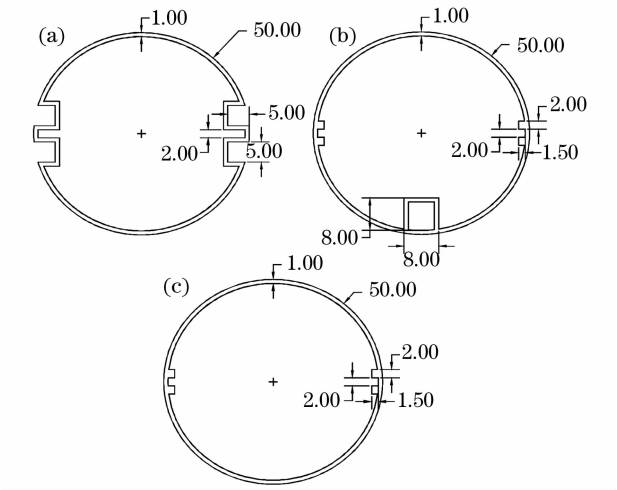

Fig. 15 Initial design of boom structures for (a) #1, (b) #2, (c) #3

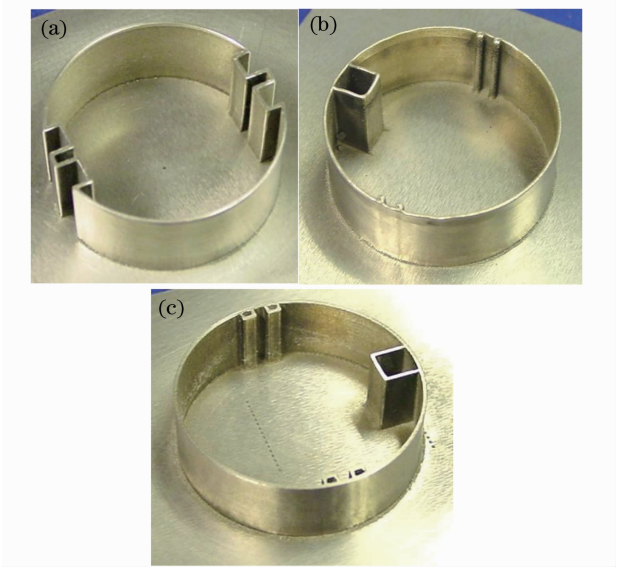

Fig. 16 Boom structures built by LC IN-625 alloy. (a) design #1; (b) design #2 with slots formed by ribs; (c) design #2 with slots formed by rectangular tubes

study reveals that LC process can be used to accommodate specific design features, prove design concepts, and provide versatile customization. Based on the design practice, the boom design #3 with an internal slot to hold an electronic board (Fig. 15 (c)) was finally selected as the boom design.

LC process was successfully used to build the test-pieces of the multi-functional boom structure capable of providing high structural stiffness, with dedicated features to support electronic driver/control cards and the data/power bus while allowing the dissipation of the heat generated by the electronic drivers. Figure 17 shows the Ti-6Al-4V boom built using LC process. The boom, about 270 mm in length and 0.8 mm in thickness, has four ribs inside to form a slot to hold electronic card. Multilayer Ti-6Al-4V cladding was applied on both ends of the boom to enhance the local areas and four Ti-6Al-4V pads were built on the clad layer at each end to enable the connections for the housing and payload, respectively. The LC Ti-6Al-4V boom is in as-consolidated surface finish, except the contact surfaces that were machined for final assembly.

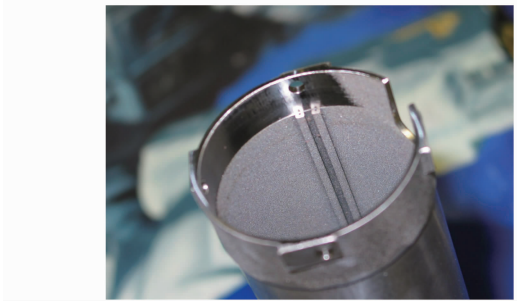

Fig. 17 LC Ti-6Al-4V boom with a slot to hold electronic card, after final machining

Conventional design of a space robot manipulator generally consists of separate booms and joint housings that are connected to each other through a flanged interface, which substantially increases the weight and complexity. One-piece integrated boom/housing design is preferrable to reduce the weight and complexity, and increase interface stiffness of a typical robotic arm. However, it is extremely difficult or even impossible to make the one-piece integrated boom/housing using conventional manufacturing processes. LC process is a free-form fabrication process that allows the building of net-shape functional features on the existing components. Therefore, it offers an unique capability to build multi-functional boom on pre-machined (or pre-built) housing for realizing the innovative design for one-piece integrated boom/housing. Figure 18 shows an integrated boom/housing manufactured using LC of Ti-6Al-4V alloy. The integrated LC Ti-6Al-4V boom/housing shows as-consolidated surface finish, except the contact surfaces that were initially machined for the next stage final machining and assembly.

The ARMS consists of four LC Ti-6Al-4V structural components:

- One Ti-6Al-4V multi-functional boom,
- Two Ti-6Al-4V housings #1 with interface,
- One Ti-6Al-4V housing #2 with integrated boom.

LC process successfully built all above components

Fig. 18　LC Ti-6Al-4V integrated boom/housing, after initial machining

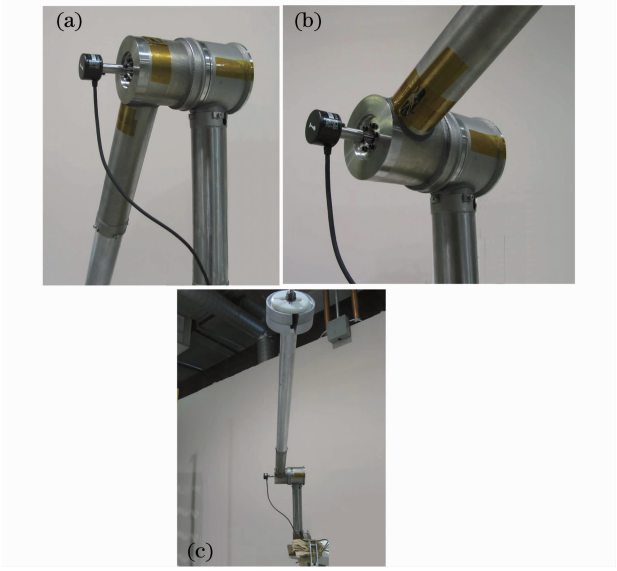

Fig. 19　Assembled ARMS with LC Ti-6Al-4V structural components. (a) and (b) close views, and (c) testing with payload

from Ti-6Al-4V alloy. The ARMS prototype robotic joint was assembled by MD Robotics using the LC Ti-6Al-4V structural components along with the other mechanical and electronic components. Figures 19(a) and (b) show close views of the assembled joint and Fig. 19(c) shows the ARMS with required payload during laboratory testing. The real time testing results demonstrated that the laser-consolidated components performed very well and all design requirements such as low weight and high strength were achieved.

4.3　Shelled Structures

NRC-IMI collaborated with several companies within the scope of Precision and Freeform Fabrication Special Interest Group (PFF-SIG) to develop LC process to build functional shell structures for parts and moulds, and investigate backfill methods to enhance the shell structures for the rapid tooling applications. An unique backfill material was developed, which has the good compression strength and thermal conductivity, and its thermal expansion is comparable with the laser consolidated shell. The backfilled shell structures can operate at relatively high working temperatures (above 350 ℃). By using the backfill method, complex cooling channels and even heating elements can be embedded into a mould (or a component) at desired locations to improve the functionality and productivity.

The possibility of using the laser-consolidated shell structure to make mould inserts was also demonstrated within the PFF-SIG. A mock mould with 5-piece inserts embedded with cooling channels was designed for demonstration. The mock mould consists of four external inserts and one core insert to form the cavity of a half FSP shell (max diameter of 54.6 mm and height of 64 mm). LC process was successfully performed to build 5 pieces of the thin-wall IN-625 alloy shell structures (Fig. 20(a)). The laser consolidated IN-625 shells were backfilled and embedded with cooling channels to form the multi-piece mould inserts for demonstration (Fig. 20(b)). Injection moulding testing was conducted on a simple-shaped, shell-based mould insert back-filled and embedded with cooling channels. Preliminary results reveal that the shell-based mould inserted with conformal cooling demonstrates much lower subsurface temperatures and, therefore, much shorter moulding cyclic time than the solid block H13 insert baseline.

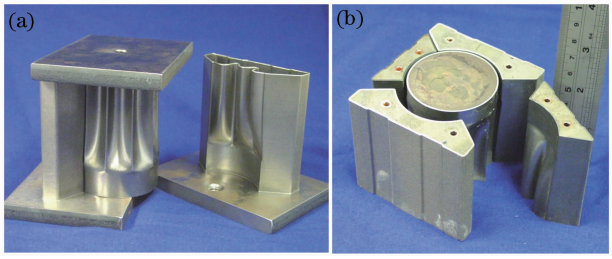

Fig. 20　Shell-based moulds for demonstration. (a) LC IN-625 shells; (b) 5-piece mould inserts embedded with cooling channels

4.4　Building Features on Pre-machined Substrate or Existing Component

LC is a material addition process that can directly build net-shape functional features on a pre-machined substrate or an existing component to form integrated structure without the need of welding or brazing, which can significantly reduce manufacturing time and material waste. Figure 21 shows a demonstration piece with the LC IN-625 fins built on pre-machined 316L stainless steel

round bar. The LC fins have as-consolidated surface finish except their top surface that was ground. If this piece is manufactured using conventional machining, it has to start from a large round bar stock and machine out majority of material to form the fins. Due to the thin wall thickness (about 0.8 mm), it will be difficult to cast these fins and also the tooling cost to make the part will be quite high for small quantity, even if it can be made by casting process. Using LC process, it can readily build the required shape, no more and no less.

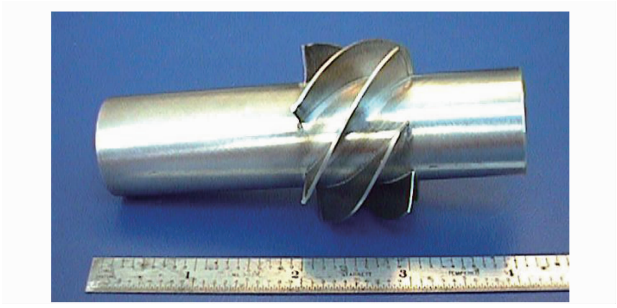

Fig. 21 LC IN-625 fins built on pre-machined 316L stainless steel shaft

Fig. 22 Demonstration impellers with LC IN-718 blades built on pre-machined substrates. Left one in as-consolidated condition, and right one after sand blasting

Figure 22 shows two IN-718 impellers manufactured by using LC process to directly build up the blades on pre-machine substrates. It is evident that this novel process produces high quality, fairly complex shapes directly from a CAD model with good surface finishes in as-consolidated condition without any further processing (as shown by the impeller on the left side). The bond between the LC blades and the pre-machined substrate is metallurgically sound, without any crack and porosity. Compared to the conventional welding process, the heat input from LC process to the substrate is minimal, resulting in a very small heat affected zone (several tens of micrometers). After sand blasting, the LC blades and pre-machined substrate show consistent surface finish (as shown by the impeller on the right side). Through the case, LC process demonstrates the potential to directly manufacture the net-shape functional impellers without moulds or dies. By using LC process, more unique features can be added to the existing components to provide additional functionality, and significantly reduce manufacturing time and cost.

5 Conclusions

In conclusion, firstly, the LC CPM-9V, IN-625, IN-718, and Ti-6Al-4V materials demonstrate the excellent mechanical properties, which enable LC process to build the functional components directly for various applications. Secondly, compared with the other laser cladding based free-form fabrication processes that only produce near-net-shape components, LC process provides an unique capability to build the net-shape functional components or features on the existing components that are difficult or even impossible to produce by using conventional manufacturing processes. LC process readily accommodates rapid design changes since no hard tooling is required. At last, LC is a green manufacturing technology that directly builds the required shapes with minimal machining. It also significantly simplifies the tooling requirements. This computer-aided manufacturing process is expected to make a huge impact on manufacturing in a wide range of industries in the near future.

Acknowledgement The author would like to thank A. Theriault, Y. Li, J. Chen, S.-H. Wang, J. Jiang, G. Campbell, A. Gillett, G. Wabersich, N. Santos, B. Gibson, J. Fenner, and M. Meinert for their numerous contributions in process development, sample preparation, and characterization. The author would also like to take this opportunity to thank many industrial collaborators (including Rotoflex, MD Robotics, Canadian Space Agency, etc.) for their strong support in developing the technology for their specific applications.

References

1 D. M. Keicher, W. D. Miller, J. E. Smugeresky *et al*.. Laser engineering net shaping (LENS™): beyond rapid prototyping to direct fabrication [C]. *Proceedings of the* 1998 *TMS Annual Meeting*, 1998. 369～377

2 J. Mazumder, J. Choi, K. Nagarathnam *et al*.. Direct metal deposition of H13 tool steel for 3-D components [J]. *JOM*, 1997, **49** (8):55～60

3 G. K. Lewis, E. Schlienger. Practical considerations and capabil-

ities for laser assisted direct metal deposition [J]. *Materials and Design*, 2000, **21**(4): 417～423
4 X. Wu, J. Mei. Near net manufacturing of components using direct laser fabrication technology [J]. *Journal of Materials Processing Technology*, 2003, **135**(2-3): 266～270
5 L. Xue, M. U. Islam. Free-form laser consolidation for producing metallurgically sound and functional components [J]. *Journal of Laser Applications*, 2000, **12**(4): 160～165
6 L. Xue, J.-Y. Chen, M. U. Islam. Functional Properties of Laser Consolidated Wear Resistant Stellite 6 Alloy [M]. Powder Metallurgy Alloys and Particulate Materials for Industrial Applications, ed. by David E. Alman and Joseph W. Newkirk, 2000. 65～74
7 L. Xue, J.-Y. Chen, M. U. Islam *et al*.. Laser consolidation of IN-738 alloy for repairing cast IN-738 gas turbine blades [C]. *Proceedings of 20th ASM Heat Treating Society Conference*, 2000. 1063～1071
8 L. Xue, J.-Y. Chen, A. Theriault. Laser consolidation of Ti-6Al-4V alloy for the manufacturing of net-shape functional components [C]. *Proceedings of 21st International Congress on Applications of Laser & Electro-Optics* (*ICALEO* 2002), 2002. 168～179
9 L. Xue, J.-Y. Chen, A. Theriault. Laser consolidation of Al 4047 alloy [C]. *Proceedings of ICALEO* 2005, 2005. 344～351
10 L. Xue, J.-Y. Chen, S-H. Wang *et al*.. Laser consolidation of waspalloy and IN-718 alloys for making net-shape functional parts for gas turbine applications [C]. *Proceedings of ICALEO* 2008, 2008. 255～263
11 L. Xue, A. Theriault, J. Chen *et al*.. Laser consolidation of CPM-9V tool steel for manufacturing rotary cutting dies [C]. *Proceedings of 10th International Symposium on Processing and Fabrication of Advanced Materials*, 2002. 361～376
12 L. Xue, A. Theriault, B. Rubinger *et al*.. Investigation of laser consolidation process for manufacturing structural components for advanced robotic mechatronics system [C]. *Proceedings of the ICALEO* 2003, 2003. 134～143
13 L. Xue, A. Theriault, M. U. Islam *et al*.. Laser consolidation of Ti-6Al-4V alloy to build functional net-shape airfoils with embedded cooling channels [C]. *Proceedings of the ICALEO* 2004, 2004. 34～40
14 L. Xue, C. Purcell. Laser consolidation of net-shape shells for flextensional sonar projectors [C]. *Proceedings of the ICALEO* 2006, 2006. 686～694
15 L. Xue, Y. Li, T. Van Daam *et al*.. Investigation of laser consolidation for manufacturing functional net-shape components for potential rocket engine applications [C]. *Proceedings of the ICALEO* 2007, 2007. 161～169
16 K. E. Pinnow, W. Stasko. P/M Tool Steel. Metals Handbook, 10th edition, Vol. 1, ASM International, Ohio: 1990. 786～789
17 Inconel Alloy 625 datasheet from Special Metals website: http://www.specialmetals.com/products/inconelalloy625.php
18 R. E. Reed-Hill. Physical Metallurgy Principles [M], 2nd Edition, New York: D. Van Nostrand Company, 1973. 581
19 G. L. Erickson. Polycrystalline Cast Superalloys. Metals Handbook, 10th Edition, Vol. 1, ASM International, Ohio: 1990. 984
20 F. R. Morral. Wrought Superalloys. Metals Handbook, 9th Edition, Vol. 3, American Society for Metals, Ohio: 1980. 219
21 A. Theriault, L. Xue, J. R. Dryden. Fatigue behaviour of laser consolidated IN-625 at room and elevated temperatures [J]. *Materials Science and Engineering A*, 2009, **516**(1-2): 217～225
22 W. L. Mankins, S. Lamb. Nickel, Nickel Alloys. ASM Handbook, Vol. 2 Properties and Selection: Nonferrous Alloys and Special-Purpose Materials, ASM International: 1990. 438
23 F. R. Morral. Wrought Superalloys. Metals Handbook (9th Edition) Volume 3 Properties and Selection: Stainless Steels, Tool Materials and Special-purpose Metals, American Society for Metals: 1980. 219
24 S. Azadian. Aspects of Precipitation in the Alloy Inconel 718 [D]. Doctoral Thesis, Lulea, Sweden: Lulea University of Technology, 2004. 15
25 Titanium Alloy Ti-6Al-4V datasheet from Carpenter Technology website: http://cartech.ides.com/datasheet.aspx? i = 101&E = 269
26 R. R. Boyer. Titanium and Titanium Alloys. ASM Handbook, Vol. 9: Metallography and Microstructures, ASM International: 1985. 458～475
27 J. R. Newman, Titanium Castings. Metals Handbook 9th Edition, Vol. 3, American Society for Metals: 1980. 409
28 ASM Committee on Titanium and Titanium Alloys. Properties of Titanium and Titanium Alloys. Metals Handbook 9th Edition, Vol. 3, American Society for Metals: 1980. 388～389
29 J. R. Davis. Titanium and Titanium Alloys. ASM Specialty Handbook: Heat-Resistant Materials, ASM International: 1997. 347～360
30 A. Theriault, L. Xue, J.-Y. Chen. Laser consolidation of Ti-6Al-4V alloy [C]. *Proceedings of the 5th International Workshop on Advanced Manufacturing Technologies* (*AMT* 2005), London, Ontario: 2005. 267～272
31 D. Eylon, J. R. Newman, J. K. Thorne. Titanium and Titanium Alloy Castings. ASM Handbook, Vol. 2: Properties and Selection: Nonferrous Alloys and Special-Purpose Materials, ASM International: 1990. 642